AIAA JOURNAL
Vol. 34, No. 6, June 1996

Improved Transient Response Approximation for General Damped Systems

A. E. Sepulveda*
University of California, Los Angeles, Los Angeles, California 90024
and
H. L. Thomas†
Structural Optimization Specialists, Santa Barbara, California 93101

A new approximation for peak transient dynamic displacements is presented. This approximation is based on modal analysis and is valid for general damped structures, which includes the case of actively controlled structures. Intermediate design variable and intermediate response quantity concepts are used to enhance the accuracy of the approximation. When this high-quality approximation is used within the context of the approximation concepts approach to design synthesis, the overall efficiency of the process expected to be improved by reducing the number of complete analyses required for convergence. Numerical results that illustrate the effectiveness of the method are presented.

Introduction

IN structural optimization, the direct solution of a synthesis problem that contains dynamic response constraints is very costly since it usually requires a large number of analyses to evaluate the constraint values. This cost is particularly high for transient dynamic analysis. The use of the approximation concepts approach is then needed for efficient structural synthesis. When using this approach, the number of design cycles needed for convergence is strongly dependent on the accuracy of the approximations used for the constrained structural responses. It is therefore important to use approximations that can accurately capture the nonlinear relationships between structural responses and the design variables.

At the early stages of the development of the approximation concepts approach, approximate representations for constraints and objective functions were generated using first-order Taylor series expansions in terms of direct or reciprocal sizing type design variables.[1,2] More accurate approximations can be constructed, however, using approximations of intermediate response quantities, which were introduced in Ref. 2, in terms of selected intermediate design variables. The intermediate response quantity idea has been applied to static stress constraints,[3] frequency constraints,[4] steady-state harmonic displacements,[5,6] control force constraints, complex eigenvalues,[7] and transient dynamic displacements.[8] A very complete survey on approximation concepts is given in Ref. 9. The approximations introduced in this paper are an extension of the undamped case presented in Ref. 8 and uses the concepts given in Ref. 7 for complex eigenvalue approximation.

In this approach, simple approximations (e.g., linear, reciprocal, and hybrid) of intermediate response quantities (e.g., forces in the case of stress constraints and modal energies in the case of frequency constraints) in terms of selected intermediate design variables can be used while retaining the explicit nonlinear dependence of the constraints on the intermediate response quantities and the explicit relationship between the intermediate design variables and the actual design variables.

Mathematically a constraint can be written as

$$g(R, x, y) \leq 0 \tag{1}$$

where $R_i, i \in I$, denote the intermediate response quantities, x_j, $j \in J$, denote the intermediate design variables, and $y_k, k = 1, \ldots,$ NDV (number of design variables), are the actual design variables.

It is assumed that 1) g is explicit in R_i, x_j, and y_k; 2) $R_i(x)$, $i \in I$, are implicit functions of x_j, $j \in J$; and 3) $x_j(y)$, $j \in J$, are explicit functions of the actual design variables y_k, $k = 1, \ldots,$ NDV.

The approximations are constructed using Taylor series expansions of R_i in terms of x_j. For example, if a linear series is used

$$\tilde{R}_i(x) = R_i(x_0) + \sum_{j \in J} \frac{\partial R_i(x_0)}{\partial x_j}(x_j - x_{j0}) \tag{2}$$

Replacing these approximations in Eq. (1), the approximation for g is then given by

$$\tilde{g}(y) = g\{\tilde{R}[x(y)], x(y), y\} \tag{3}$$

In the case of transient response of damped structures, small changes in the design variables can lead to large changes in the amplitude of the dynamic response and the times at which peak responses occur. In this paper, an approximation for peak transient response of general damped structures, which captures most of the inherent nonlinearities, is introduced. This approximation is based on the modal solution of the equations of motion and makes extensive use of the concepts of intermediate response quantities and intermediate design variables.

Dynamic Response

The general matrix equation of motion for a damped structure is given by

$$[M]\{\ddot{u}\} + [C]\{\dot{u}\} + [K]\{u\} = \{p\} \tag{4}$$

where $[M]$, $[C]$, and $[K]$ are the $n \times n$ mass, viscous damping, and stiffness matrices, respectively. The matrices $[C]$ and $[K]$ will be considered nonsymmetric to include the case of general actively controlled structures. The term $\{p\}$ is the vector of applied loads, $\{u\}$ is the vector of dynamic displacements and rotations, and n denotes the number of degrees of freedom for the system.

Modal Analysis

Defining the state space variables as

$$\{q\} = \begin{Bmatrix} \{\dot{u}\} \\ \{u\} \end{Bmatrix} \tag{5}$$

Received Jan. 27, 1995; revision received July 28, 1995; accepted for publication July 28, 1995.

*Assistant Professor, Department of Mechanical, Aerospace and Nuclear Engineering. Member AIAA.
†Owner. Member AIAA.

Equation (4) leads to the equations of motion in first-order form, namely,

$$[M^*]\{\dot{q}\} + [K^*]\{q\} = \{P\} \tag{6}$$

where

$$[M^*] = \begin{bmatrix} [0] & [M] \\ [M] & [C] \end{bmatrix} \tag{7a}$$

$$[K^*] = \begin{bmatrix} -[M] & [0] \\ [0] & [K] \end{bmatrix} \tag{7b}$$

and

$$\{P\} = \begin{Bmatrix} \{0\} \\ \{p\} \end{Bmatrix} \tag{7c}$$

Consider the following eigenproblems associated with Eq. (6),

Right eigenproblem:

$$(\lambda[M^*] + [K^*])\{\phi\} = \{0\} \tag{8a}$$

Left eigenproblem:

$$\{\chi\}^T(\lambda[M^*] + [K^*]) = \{0\}^T \tag{8b}$$

The solution of these eigenproblems leads to $2n$ complex conjugate eigenvalues $\lambda_1, \ldots, \lambda_{2n}$ and the associated complex conjugate right and left eigenvectors $\{\phi\}_1, \ldots, \{\phi\}_{2n}$ and $\{\chi\}_1, \ldots, \{\chi\}_{2n}$. The right and left eigenvectors are orthogonal with respect to the $[M^*]$ and $[K^*]$ matrices, i.e.,

$$\{\chi\}_i^T[M^*]\{\phi\}_j = 0 \quad \text{if} \quad i \neq j \quad i, j = 1, \ldots, 2n \tag{9a}$$

$$\{\chi\}_i^T[K^*]\{\phi\}_j = 0 \quad \text{if} \quad i \neq j \quad i, j = 1, \ldots, 2n \tag{9b}$$

For convenience, the following numbering for eigenvalues is assumed:

$$\lambda_i = \sigma_i + j\omega_{di} \qquad i = 1, \ldots, n \tag{10a}$$

$$\lambda_{n+i} = \bar{\lambda}_i \qquad i = 1, \ldots, n \tag{10b}$$

where the real part σ_i denotes damping and the imaginary part ω_{di} is the damped frequency for mode i. The notation $\bar{z}$ is used for complex conjugate, i.e., if $z = a + jb$, then $\bar{z} = a - jb$ ($j = \sqrt{-1}$). The modes are ordered in ascending order of the damped frequencies ($\omega_{d1} < \omega_{d2} < \ldots \omega_{dn}$). Also for eigenvectors

$$\{\phi\}_{n+i} = \{\bar{\phi}\}_i \qquad i = 1, \ldots, n \tag{11a}$$

$$\{\chi\}_{n+i} = \{\bar{\chi}\}_i \qquad i = 1, \ldots, n \tag{11b}$$

The complex eigenvectors can be partitioned in velocity and position parts as

$$\{\phi\}_i = \begin{Bmatrix} \{\phi_v\} \\ \{\phi_p\} \end{Bmatrix}_i \tag{12a}$$

$$\{\chi\}_i = \begin{Bmatrix} \{\chi_v\} \\ \{\chi_p\} \end{Bmatrix}_i \tag{12b}$$

The velocity and position parts are related such that[7]

$$\{\phi_v\}_i = \lambda_i\{\phi_p\}_i \tag{13a}$$

$$\{\chi_v\}_i = \lambda_i\{\chi_p\}_i \tag{13b}$$

and with this notation, the right and left eigenvectors are normalized such that

$$\{\phi_p\}_i^T[M]\{\phi_p\}_i = 1 \qquad i = 1, \ldots, 2n \tag{14a}$$

$$\{\chi_p\}_i^T[M]\{\phi_p\}_i = 1 \qquad i = 1, \ldots, 2n \tag{14b}$$

In this paper, the modal solution of the dynamic response problem will be used. In the modal solution approach, it is assumed that the dynamic state space response can be represented as a linear combination of complex mode shapes of the form

$$\{q\} = \sum_{i=1}^{2n} \{\phi\}_i \eta_i(t) \tag{15}$$

Substituting Eq. (15) in Eq. (6), premultiplying by $\{\chi\}_r^T$, and using the orthogonality of left and right eigenvectors [Eqs. (9)] lead to

$$T_r^*\dot{\eta}_r(t) + U_r^*\eta_r(t) = \{\chi\}_r^T\{P\} \tag{16}$$

where

$$T_r^* = \{\chi\}_r^T[M^*]\{\phi\}_r \tag{17a}$$

$$U_r^* = \{\chi\}_r^T[K^*]\{\phi\}_r \tag{17b}$$

and from the definition of T_r^* and U_r^* and Eqs. (8), it is easily seen that

$$\lambda_r = -U_r^*/T_r^* \tag{18}$$

and therefore, Eq. (16) can be written as

$$\dot{\eta}_r(t) - \lambda_r\eta_r(t) = \frac{\{\chi\}_r^T\{P\}}{T_r^*} \tag{19}$$

Using the definition of T_r^* and U_r^* [Eqs. (17)] and the relation between velocity and position parts of the eigenvectors [Eqs. (13)], the following identities are obtained:

$$T_r^* = 2\lambda_r T_r + S_r \tag{20a}$$

$$U_r^* = -\lambda_r^2 T_r + U_r \tag{20b}$$

where T_r, U_r, and S_r are the modal energies (introduced in Ref. 7) given by

$$T_r = \{\chi_p\}_r^T[M]\{\phi_p\}_r \tag{21a}$$

$$U_r = \{\chi_p\}_r^T[K]\{\phi_p\}_r \tag{21b}$$

and

$$S_r = \{\chi_p\}_r^T[C]\{\phi_p\}_r \tag{21c}$$

Using the definition of $\{P\}$ given in Eq. (7c) gives

$$\{\chi\}_r^T\{P\} = \{\chi_p\}_r^T\{p\} \tag{22}$$

Introducing Eqs. (20a) and (22) into Eq. (19), the differential equations for the modal participation coefficients are then given by

$$\dot{\eta}_r(t) - \lambda_r\eta_r(t) = \frac{\{\chi_p\}_r^T\{p\}}{2\lambda_r T_r + S_r} \qquad r = 1, \ldots, 2n \tag{23}$$

Clearly, these coefficients also appear in complex conjugate pairs, i.e.,

$$\eta_{n+r}(t) = \bar{\eta}_r(t), \qquad r = 1, \ldots, n$$

Initial Conditions

Assuming for the moment, that the functions $\eta_r(t)$ are known, consider the response given by Eq. (15) at the initial time $t = t_0$ (usually $t_0 = 0$)

$$\{q_0\} = \sum_{i=1}^{2n} \{\phi\}_i \eta_r(t_0) \tag{24}$$

and premultiplying Eq. (24) by $\{\chi\}_r^T[M^*]$ leads to

$$\eta_r(t_0) = \frac{\{\chi\}_r^T[M^*]\{q_0\}}{T_r^*} \tag{25}$$

or, using Eqs. (5), (12b), and (20a),

$$\eta_r(t_0) = \frac{\lambda_r\{\chi_p\}_r^T[M]\{u_0\} + \{\chi_p\}_r^T[C]\{u_0\} + \{\chi_p\}_r^T[M]\{\dot{u}_0\}}{2\lambda_r T_r + S_r} \tag{26}$$

where $\{u_0\}$ and $\{\dot{u}_0\}$ denote the initial displacements and velocities.

Defining the complex quantities[8]

$$TV_r = \{\chi_p\}_r^T[M]\{\dot{u}_0\} \tag{27a}$$

$$TD_r = \{\chi_p\}_r^T[M]\{u_0\} \tag{27b}$$

$$SD_r = \{\chi_p\}_r^T[C]\{u_0\} \tag{27c}$$

the initial condition for η_r [Eq. (26)] can be written as

$$\eta_r^0 \equiv \eta_r(t_0) = \frac{\lambda_r TD_r + SD_r + TV_r}{2\lambda_r T_r + S_r} \tag{28}$$

Load Case

The general solution to Eq. (23) with the initial condition at $t = t_0$ given by Eq. (28) is given by

$$\eta_r(t) = e^{\lambda_r(t-t_0)}\eta_r^0 + \int_{t_0}^{t} \frac{e^{\lambda_r(t-\zeta)}\{\chi_p\}_r^T\{p(\zeta)\}}{2\lambda_r T_r + S_r}\mathrm{d}\zeta \tag{29}$$

If general load vectors ($\{p(t)\}$) are considered, numerical integration of Eq. (29) is unavoidable to obtain $\eta_r(t)$. To alleviate this computational burden and obtain closed-form solutions, an explicit representation for the load vector is assumed. In this work, two cases will be examined. The first case, introduced in Ref. 8, expresses the load vector as a truncated Fourier series of the form

$$\{p(t)\} = \begin{cases} \sum_n (\{p_{ns}\}\sin\Omega_n t + \{p_{nc}\}\cos\Omega_n t) & \text{if} \quad t_0 \le t \le t_1 \\ \{0\} & \text{if} \quad t_1 < t \le t_f \end{cases} \tag{30}$$

where $\{p_{ns}\}$ and $\{p_{nc}\}$ are coefficient vectors of sine and cosine components, respectively, and the various Ω_n are the forcing frequencies. The foregoing expression indicates that the load is only applied during the time interval $t_0 \le t \le t_1$ and for $t > t_1$, the structure is unloaded. Furthermore, it is assumed that the total time period $t_0 \le t \le t_f$ is the analysis interval of interest. The representation given by Eq. (30) will, in general, reduce the number of terms needed for the Fourier representation of general loads. It is important to note that further subdivision of the time interval is possible, but only one is used in this work for simplicity.

The solution to Eq. (23) with the load representation given by Eq. (30) is given by

$$\eta_r(t) = \begin{cases} e^{\lambda_r(t-t_0)}\left[\eta_r^0 - z_r(t_0)\right] + z_r(t) & \text{if} \quad t_0 \le t \le t_1 \\ e^{\lambda_r(t-t_0)}\left[\eta_r^0 - z_r(t_0)\right] + e^{\lambda_r(t-t_1)}z_r(t_1) & \text{if} \quad t_1 < t \le t_f \end{cases} \tag{31}$$

where η_r^0 is given by Eq. (28) and $z_r(t)$ by

$$z_r(t) = \sum_n (a_{rn}\sin\Omega_n t + b_{rn}\cos\Omega_n t) \tag{32}$$

and

$$a_{rn} = \frac{-\lambda_r\{\chi_p\}_r^T\{p_{ns}\} + \Omega_n\{\chi_p\}_r^T\{p_{nc}\}}{(2\lambda_r T_r + S_r)\left(\lambda_r^2 + \Omega_n^2\right)} \tag{33a}$$

$$b_{rn} = \frac{-\Omega_n\{\chi_p\}_r^T\{p_{ns}\} - \lambda_r\{\chi_p\}_r^T\{p_{nc}\}}{(2\lambda_r T_r + S_r)\left(\lambda_r^2 + \Omega_n^2\right)} \tag{33b}$$

The second case is more general and assumes that the load vector is piecewise linear in time (see Fig. 1). The analysis time interval $[t_0, t_f]$ is subdivided such that $t_0 < t_1 < \cdots < t_m = t_f$. The load vector is specified at each time t_i, $\{p(t_i)\}$, $i = 0, \ldots, m$. Thus, for the interval $[t_i, t_{i+1}]$, the forcing vector is given by

$$\{p(t)\} = \{a_i\} + \{b_i\}t \qquad t \in [t_i, t_{i+1}] \tag{34a}$$

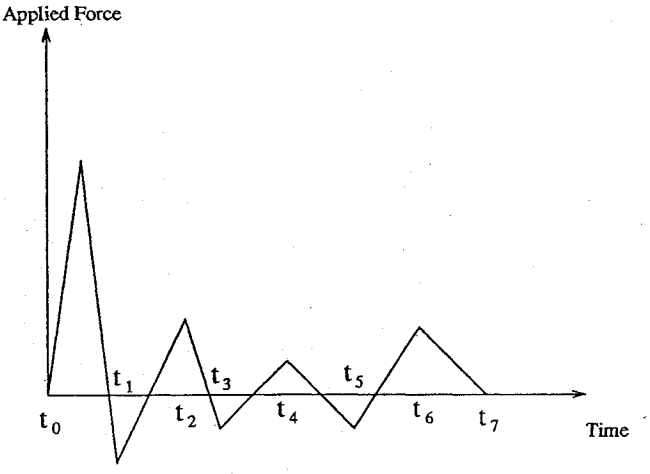

Fig. 1 Piecewise linear representation of external loads.

where

$$\{a_i\} = \frac{\{p(t_i)\}t_{i+1} - \{p(t_{i+1})\}t_i}{t_{i+1} - t_i} \tag{34b}$$

$$\{b_i\} = \frac{\{p(t_{i+1})\} - \{p(t_i)\}}{t_{i+1} - t_i} \tag{34c}$$

The solution for $\eta_r(t)$, for the load representation given by Eqs. (34), in the time interval $[t_i, t_{i+1}]$ is denoted by $\eta_r^{(i)}(t)$, and it is given by

$$\eta_r^{(i)}(t) = e^{\lambda_r(t-t_i)}\left[\eta_r^{(i-1)}(t_i) - \alpha_r^{(i)} - \beta_r^{(i)}t_i\right] + \alpha_r^{(i)} + \beta_r^{(i)}t \qquad t \in [t_i, t_{i+1}] \tag{35a}$$

where

$$\alpha_r^{(i)} = \frac{-\{\chi_p\}_r(\{b_i\} - \lambda_r\{a_i\})}{\lambda_r^2(2\lambda_r T_r + S_r)} \tag{35b}$$

$$\beta_r^{(i)} = \frac{-\{\chi_p\}_r^T\{b_i\}}{\lambda_r(2\lambda_r T_r + S_r)} \tag{35c}$$

Equation (35a) gives a recursive formula to evaluate $\eta_r^{(i)}(t)$ for each interval $[t_i, t_{i+1}]$. Recognizing that $\eta_r^{(0)}(t_0) = \eta_r^0$, given in Eq. (28), the participation coefficients $\eta_r^{(i)}$, $i = 1, \ldots, m$, are obtained directly from Eqs. (35).

Finally, from Eq. (15) and using the fact that the complex eigenvectors appear in complex conjugate pairs, the vector of dynamic displacements is given by

$$\{u(t)\} = 2\,\mathrm{Re}\left(\sum_{i=1}^{n}\{\phi_p\}_i\eta_i(t)\right) \tag{36}$$

where $\eta_i(t)$, $i = 1, \ldots, n$, is given by Eqs. (31) or (35), depending on the load representation selected.

Undamped Case

If there is no damping in the system, from Eqs. (8) it is easily seen that

$$\lambda_r = \pm j\omega_r \tag{37a}$$

and with the normalization given by Eqs. (14),

$$\{\chi_p\}_r = \{\phi_p\}_r = \{\phi_n\}_r \tag{37b}$$

where ω_r and $\{\phi_n\}_r$ are the rth natural frequency and natural mode shape for the structure. Introducing Eq. (37b) into Eq. (36), the displacement vector for this case is given by

$$\{u(t)\} = 2\,\mathrm{Re}\left(\sum_{i=1}^{n}\{\phi_n\}_i\eta_i(t)\right) = \sum_{i=1}^{n}\{\phi_n\}_i\,\mathrm{Re}[2\eta_i(t)] \tag{38}$$

since the natural mode shapes are real vectors. Equation (23), for the undamped case, becomes

$$\dot{\eta}_r(t) - j\omega_r\eta_r(t) = -j\frac{\{\phi_n\}_r^T\{p\}}{2\omega_r T_r} \tag{39}$$

separating real and imaginary parts for $\eta_r(t)$ as

$$\eta_r(t) = \eta_r^{(R)}(t) + j\eta_r^{(I)}(t) \tag{40}$$

and introducing this relation in Eq. (39), the differential equations for real and imaginary parts are given by

$$\dot{\eta}_r^{(R)}(t) + \omega_r\eta_r^{(I)}(t) = 0 \tag{41a}$$

$$\dot{\eta}_r^{(I)}(t) - \omega_r\eta_r^{(R)} = -\frac{\{\phi_n\}_r^T\{p\}}{2\omega_r T_r} \tag{41b}$$

differentiating Eq. (41a) and replacing $\dot{\eta}_r^{(I)}(t)$ from Eq. (41b), the differential equation for $\eta_r^{(R)}(t)$ is given by

$$\ddot{\eta}_r^{(R)}(t) + \omega_r^2\eta_r^{(R)}(t) = \frac{\{\phi_n\}_r^T\{p\}}{2T_r} \tag{42}$$

then, defining

$$z_r(t) = 2Re[\eta_r(t)] = 2\eta_r^{(R)}(t) \tag{43}$$

Eq. (42) becomes

$$\ddot{z}_r(t) + \omega_r^2 z_r(t) = \frac{\{\phi_n\}_r^T\{p\}}{T_r} \tag{44}$$

and Eq. (44) represents the usual second-order differential equation for the modal participation coefficients for the undamped case. This equation is usually modified, to include modal damping, as

$$\ddot{z}_r + 2\xi_r\omega_r\dot{z}_r + \omega_r^2 z_r = \frac{\{\phi_n\}_r^T\{p\}}{T_r} \tag{45}$$

and finally the dynamic displacements are given by [Eq. (38)]

$$\{u(t)\} = \sum_{i=1}^{n}\{\phi_n\}_i z_i(t)$$

Approximation For Dynamic Displacements

In Ref. 5, it was shown that for the case of undamped harmonic response, a high-quality approximation could be generated by approximating the modal energies T_r, U_r, and S_r in Taylor series. These basic concepts can be extended in a straightforward manner for the transient response case. For this case, the position parts of the right and left complex eigenvectors are assumed to be invariant. From this basic assumption, a high-quality approximation for the complex eigenvalues can be generated by looking at the second-order eigenproblem[6]:

$$\lambda_r^2 T_r + \lambda_r S_r + U_r = 0 \tag{46}$$

Solving for λ_r from Eq. (46) yields

$$\lambda_r = \frac{-S_r \pm \sqrt{S_r^2 - 4T_r U_r}}{2T_r} \tag{47}$$

Equation (47) has two complex conjugate solutions, which, from Eq. (47), can be written as

$$\lambda_r = \sigma_r \pm j\omega_{dr} \tag{48}$$

Comparing Eqs. (47) and (48), for underdamped modes,

$$\sigma_r = -S_r/2T_r \tag{49a}$$

$$\omega_{dr} = \sqrt{(U_r/T_r) - (S_r/2T_r)^2} \tag{49b}$$

The complex modal energies T_r, S_r, and U_r are chosen as intermediate response quantities and are approximated in Taylor series with respect to selected intermediate response quantities as

$$\tilde{T}_r = T_{r0} + \sum_j \frac{\partial T_r(x_0)}{\partial x_j}(x_j - x_{j0}) \tag{50a}$$

$$\tilde{U}_r = U_{r0} + \sum_j \frac{\partial U_r(x_0)}{\partial x_j}(x_j - x_{j0}) \tag{50b}$$

$$\tilde{S}_r = S_{r0} + \sum_j \frac{\partial S_r(x_0)}{\partial x_j}(x_j - x_{j0}) \tag{50c}$$

The partial derivatives used in the approximations are evaluated assuming that the position parts of the eigenvectors are invariant, i.e.,

$$\frac{\partial T_r}{\partial x_j} = \{\chi_p\}_r^T\frac{\partial[M]}{\partial x_j}\{\phi_p\}_r \tag{51a}$$

$$\frac{\partial U_r}{\partial x_j} = \{\chi_p\}_r^T\frac{\partial[K]}{\partial x_j}\{\phi_p\}_r \tag{51b}$$

$$\frac{\partial S_r}{\partial x_j} = \{\chi_p\}_r^T\frac{\partial[C]}{\partial x_j}\{\phi_p\}_r \tag{51c}$$

The complex eigenvalues are then approximated as

$$\tilde{\sigma}_r = -\tilde{S}_r/2\tilde{T}_r \tag{52a}$$

$$\tilde{\omega}_{dr} = \sqrt{(\tilde{U}_r/\tilde{T}_r) - (\tilde{S}_r/2\tilde{T}_r)^2} \tag{52b}$$

and

$$\tilde{\lambda}_r = \tilde{\sigma}_r \pm j\tilde{\omega}_{dr} \tag{52c}$$

Introducing the previous approximation in Eq. (29) [or Eqs. (31) and (35) for the particular forcing functions],

$$\tilde{\eta}_r(t) = e^{\tilde{\lambda}_r(t-t_0)}\tilde{\eta}_r^0 + \int_{t_0}^{t}\frac{e^{\tilde{\lambda}_r(t-\zeta)}\{\chi_p\}_r^T\{p(\zeta)\}\,d\zeta}{2\tilde{\lambda}_r\tilde{T}_r + \tilde{S}_r} \tag{53}$$

To approximate η_r^0 [see Eq. (28)], the quantities TD_r, SD_r, and TV_r [Eqs. (27)] are chosen as additional intermediate response quantities. These intermediate responses are approximated in a similar manner as T_r, U_r, and S_r, assuming that the position parts of the complex eigenvectors are invariant. The initial conditions $\{u_0\}$ and $\{\dot{u}_0\}$ are considered constant in this work but can also be considered as functions of the design variables and approximated (for example $\{u_0\}$ may represent a static equilibrium position). With these approximations $\tilde{\eta}_r^0$ is given by

$$\tilde{\eta}_r^0 = \frac{\tilde{\lambda}_r\widetilde{TD}_r + \widetilde{SD}_r + \widetilde{TV}_r}{2\tilde{\lambda}_r\tilde{T}_r + \tilde{S}_r} \tag{54}$$

Finally, the approximation for the vector of transient dynamic displacements is constructed using Eq. (36) with a truncated set of modes and the approximate modal participation coefficients given by Eq. (53)

$$\{\tilde{u}(t)\} = 2\,\mathrm{Re}\left(\sum_{i=1}^{N}\{\phi_p\}_i\tilde{\eta}_i(t)\right) \tag{55}$$

where N denotes the retained number of modes.

In summary, the quantities T_r, S_r, U_r, TV_r, TD_r, and SD_r for all retained modes are chosen as intermediate response quantities, and they are approximated to first order in terms of appropriate intermediate design variables, assuming that the eigenvectors $\{\phi_p\}_r$ and $\{\chi_p\}_r$ remain invariant. For simplicity, Eq. (36) can be written as

$$\{u(t)\} = \{u([R], t)\} \tag{56}$$

where $\{R\}$ is the vector of intermediate response quantities. Then the approximate displacement as a function of time is given by

$$\{\tilde{u}(t)\} = \{u(\{\tilde{R}\}, t)\} \tag{57}$$

Peak Time Approximation

Since transient displacements are functions of time, in an optimization environment, constraints on these quantities have to be imposed at peak times, and multiple peaks should be considered to capture peak time switching.

Peak times change when the design changes; therefore, they can also be approximated to improve the accuracy of the peak displacement approximations. If t_p denotes a peak time for the jth constrained degree of freedom (at the base design), the approximate peak displacement is given by

$$\tilde{u}_j = u_j(\{\tilde{R}\}, \tilde{t}_p) \tag{58}$$

where $\tilde{t}_p$ denotes the approximate peak time.

In this paper, the following alternative approximations for t_p are studied:

1) t_p invariant for approximate peak displacements (i.e., $\tilde{t}_p = t_p$).

2) t_p approximated explicitly in terms of the damped frequencies,

$$\frac{1}{\tilde{t}_p} = \frac{1}{t_p} - \frac{1}{t_p^2} \sum_{i=1}^{N} \frac{\partial t_p}{\partial \omega_{di}} (\omega_{di} - \omega_{d0i}) \tag{59}$$

where ω_{d0i} denotes the ith damped frequency at the base design. The expression (59) is exact if the dynamic displacement is a combination of simple harmonics.

The sensitivities in Eq. (59) are calculated by implicit differentiation of the following equation:

$$\dot{u}[\omega_d, t_p(\omega_d)] = 0 \tag{60}$$

which states that at displacement peak times, for the jth constrained degree of freedom, the velocity is zero. Differentiating Eq. (60) with respect to ω_{dk} gives

$$\frac{\partial t_p}{\partial \omega_{dk}} = \frac{\partial \dot{u}_j}{\partial \omega_{dk}} \Big/ \ddot{u}_j \tag{61}$$

where $\dot{u}_j$ and $\ddot{u}_j$ are easily obtained from Eq. (36).

3) Use a local search to find the peak time of the approximate displacement [Eq. (57)] starting from t_p to obtain $\tilde{t}_p$.

The peak times t_p for the base design can be obtained using the adaptive search method described in Ref. 10.

Direct Solution

In this section the approximation for dynamic displacements based on direct solution of Eq. (4) will be reviewed to compare it with the approximation based on modal analysis introduced previously.

The sensitivity of the dynamic displacement vector $\{u(t)\}$ with respect to a design variable y_k is obtained differentiating Eq. (4):

$$[M]\frac{\partial\{\ddot{u}\}}{\partial y_k} + [C]\frac{\partial\{\dot{u}\}}{\partial y_k} + [K]\frac{\partial\{u\}}{\partial y_k} = \{F(t)\} \tag{62}$$

where

$$\{F(t)\} = \frac{\partial\{P\}}{\partial y_k} - \frac{\partial[M]}{\partial y_k}\{\ddot{u}\} - \frac{\partial[C]}{\partial y_k}\{\dot{u}\} - \frac{\partial[K]}{\partial y_k}\{u\} \tag{63}$$

Equations (4) and (62) have the same structure and can be solved using numerical integration or modal analysis. When direct solution is used, the displacement at peak times is approximated using first-order Taylor series (linear, reciprocal, or hybrid). If, for example, linear approximations are used, for the jth degree of freedom at peak time t_p,

$$\tilde{u}_j = u_j(t_p) + \sum_{k=1}^{NDV} \frac{\partial u_j(t_p)}{\partial y_k}(y_k - y_{k0}) \tag{64}$$

An alternative approximation of this type is to use intermediate design variables instead of the actual design variables for the first-order expansion.

The proposed modal approximation given in the previous section retains most of the inherent nonlinearities of the peak transient displacement as a function of the design variables. In fact, the only approximate quantities are the intermediate response quantities T_r, U_r, S_r [see Eqs. (50)], TD_r, SD_r, and TV_r [see Eqs. (27)]. The approximation of these quantities assumes that the position parts of both left and right eigenvectors are invariant, which makes sensitivity calculations very inexpensive from a computational point of view.

On the other hand, a first-order approximation such as in Eq. (64) requires the solution of Eq. (62) to obtain the sensitivities. This equation has to be solved either in closed form using a modal approach or using some numerical integration technique. Thus, the modal approximation is in fact much less intensive numerically to construct than simple first-order approximations.

For optimization purposes, the comparison, from a computational point of view, must consider both the cost of constructing the approximation and the evaluation of the approximate displacements for each design cycle. For the example problems presented in this paper, the CPU time per design cycle using both types of approximations is very similar, but the number of analyses for convergence is greatly reduced using the modal approach.

Numerical Examples

The following examples show the effect of the proposed modal approximation in an optimization context. For the computational implementation, the approximate design problems were solved using DOT.[11]

Problem 1: Cantilever Beam

The first example is the minimum weight design of the cantilever beam shown in Fig. 2. The beam is modeled with 10 beam-type finite elements each 1.0 m in length. The motion of the beam is constrained such that only vertical displacements and in-plane rotations are allowed. A concentrated mass of 200 kg is located at the midspan node and a vertical half-sine pulse (see Fig. 2) is applied at the tip. The time period for analysis is $0 \leq t \leq 2.0$ s. For the transient dynamic analysis, the first 20 out of the total of 40 complex modes were retained. Stepwise move limits of 60% were imposed on the design variables. The vertical displacement at the tip of the beam is constrained to be less than or equal to 5.0 cm. The design variables are T_b and T_h for each beam element, with initial design $T_b = T_h = 5.0$ cm and side constraints $T_b, T_h \geq 0.5$ cm. The cross-sectional areas and inertias are used as intermediate design variables for structural elements.

Case 1: Homogeneous Initial Conditions

In this first case, initial ($t = 0$) displacements and velocities are zero for the entire length of the beam. Three runs were made for this problem, each one corresponding to the three different peak time approximation options suggested in the paper.

The iteration history data are plotted in Fig. 3, and the final designs are given in Table 1. In all four cases the peak displacement constraint is active at $t = 0.096$ s. In all cases the final design has similar characteristics, with T_h decreasing to lower bound towards the free end of the beam and T_b at lower bound. From Fig. 3 it is observed that for this problem, the convergence characteristics for all three peak time approximation schemes is very similar. To compare the performance of the modal approximation with simple first-order approximations, the problem was also solved using linear, reciprocal, and hybrid approximations with 60% move limits. None of the three cases converged within 25 design cycles, and thus move limits between 20 and 50% were used for each one. For the linear case, none of the runs converged, for the reciprocal case convergence was obtained using 20% move limits in 21 design cycles, and for the hybrid case (which is the most conservative of the three[12]) convergence was obtained with 50% move limits in 16 design cycles. The iteration histories for these cases are shown in Fig. 3 and the final designs in Table 1. These results show that the more accurate improved modal approximations require less analyses for convergence since this allows the use of larger move limits and

Table 1 Final designs of cantilever beam, case 1

Element no.	Design variables, cm	Modal approx. 60% M.L. Peak time approximation type 1	2	3	Reciprocal approx. 20% M.L.	Hybrid approx. 50% M.L.
1	T_b	3.00	3.02	2.95	3.99	3.97
	T_h	0.50	0.50	0.50	0.50	0.50
2	T_b	2.59	2.59	2.60	3.21	3.21
	T_h	0.50	0.50	0.50	0.50	0.50
3	T_b	2.17	2.14	2.16	2.47	2.47
	T_h	0.50	0.50	0.50	0.50	0.50
4	T_b	1.79	1.76	1.82	1.79	1.78
	T_h	0.50	0.50	0.50	0.50	0.50
5	T_b	1.44	1.46	1.49	1.22	0.77
	T_h	0.50	0.50	0.50	0.50	0.50
6	T_b	1.18	1.19	1.19	0.81	0.62
	T_h	0.50	0.50	0.50	0.50	0.50
7	T_b	0.85	0.90	0.88	0.59	0.50
	T_h	0.50	0.50	0.50	0.50	0.50
8	T_b	0.58	0.59	0.58	0.50	0.50
	T_h	0.50	0.50	0.50	0.50	0.50
9	T_b	0.50	0.50	0.50	0.50	0.50
	T_h	0.50	0.50	0.50	0.50	0.50
10	T_b	0.50	0.50	0.50	0.50	0.50
	T_h	0.50	0.50	0.50	0.50	0.50
Mass, kg		427	427	427	447	447
Number of analyses		8	8	8	22	17

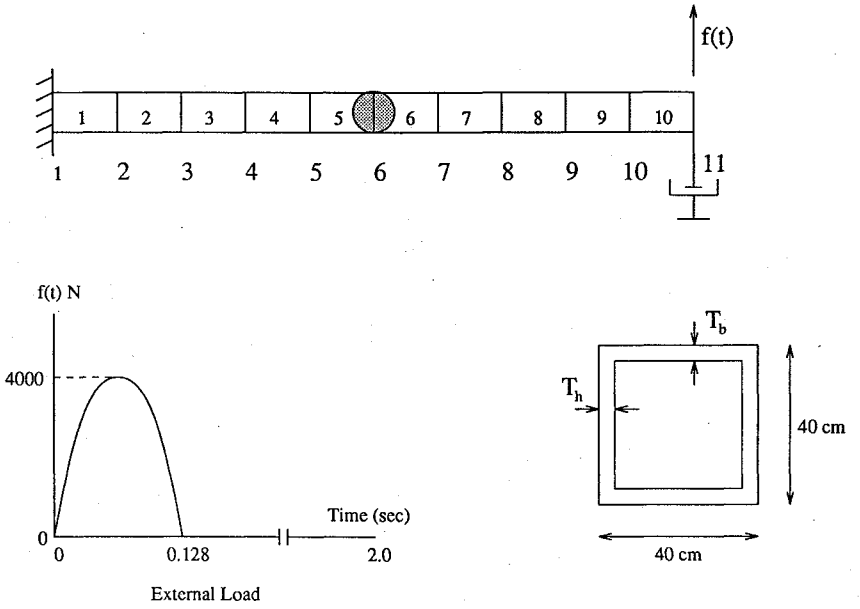

Fig. 2 Cantilever beam, problem 1.

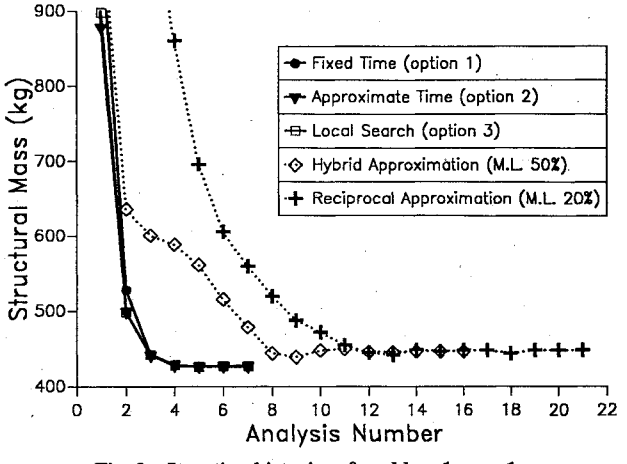

Fig. 3 Iteration histories of problem 1, case 1.

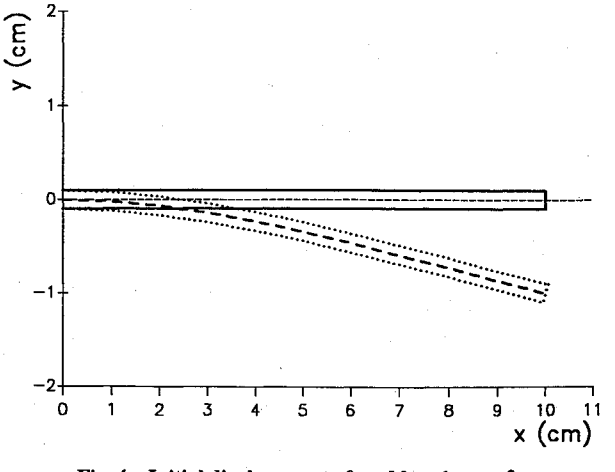

Fig. 4 Initial displacement of problem 1, case 2.

Table 2 Final designs of cantilever beam, case 2

Element no.	Design variables, cm	Modal approx. 60% M.L. Peak time approximation type 1	2	3	Reciprocal approx. 40% M.L.	Hybrid approx. 40% M.L.
1	T_b	4.24	3.75	3.37	3.78	4.12
	T_h	0.59	0.50	0.50	0.50	0.50
2	T_b	3.22	3.11	3.07	2.98	3.41
	T_h	0.50	0.50	0.50	0.50	0.50
3	T_b	2.74	2.52	2.63	2.55	2.62
	T_h	0.50	0.50	0.50	0.50	0.50
4	T_b	2.09	2.16	2.23	2.15	2.32
	T_h	0.50	0.50	0.50	0.50	0.50
5	T_b	1.63	1.80	1.79	1.82	1.85
	T_h	0.50	0.50	0.50	0.50	0.50
6	T_b	1.23	1.42	1.49	1.48	1.11
	T_h	0.50	0.50	0.50	0.50	0.50
7	T_b	0.92	1.09	1.14	1.14	0.82
	T_h	0.50	0.50	0.50	0.50	0.50
8	T_b	0.73	0.72	0.75	0.58	0.63
	T_h	0.59	0.50	0.50	0.50	0.50
9	T_b	0.52	0.50	0.50	0.50	0.50
	T_h	0.51	0.50	0.50	0.50	0.50
10	T_b	0.50	0.50	0.50	0.50	0.55
	T_h	0.50	0.50	0.50	0.50	0.54
Mass, kg		499	491	488	488	499
Number of analyses		10	9	9	20	13

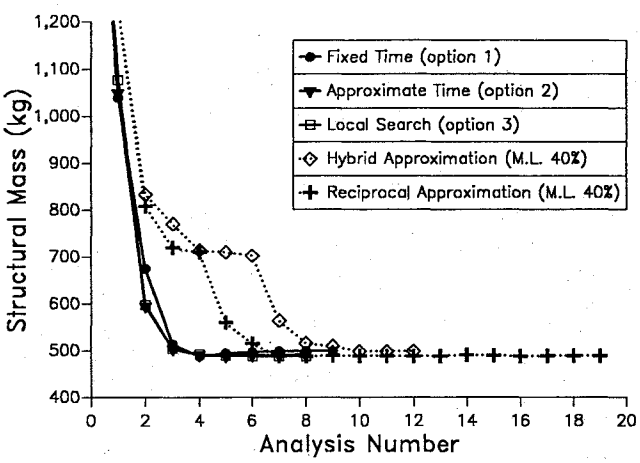

Fig. 5 Iteration histories of problem 1, case 2.

also gives a design with a final mass 4% smaller than using simple first-order approximations.

Case 2: Nonhomogeneous Initial Conditions

For this second case, a prescribed initial displacement is imposed, with homogeneous velocity initial condition. The prescribed displacement is shown in Fig. 4 and represents the deflection of the first natural mode with a displacement of 1 cm at the tip.

The iteration history data are plotted in Fig. 5, and the final designs are given in Table 2. The problem was also solved using simple first-order approximations. As in case 1, no convergence was achieved using linear approximations, whereas the reciprocal and hybrid cases converged with 40% move limits in 19 and 12 design cycles, respectively.

Problem 2: Antenna Structure

The mass minimization of an idealized antenna structure is chosen as the second example problem (see Fig. 6). It consists of eight aluminum beams ($E = 7.3 \times 10^6$ N/cm^2, $\rho = 2.77 \times 10^{-3}$ kg/cm^3, $v = 0.325$) that have thin-walled hollow box beam cross sections. The structure is constrained to move vertically only, so that each nodal point has three degrees of freedom (translation in the y direction and rotation about the x and z reference axes shown in Fig. 6)

Table 3 Final designs of antenna structure

Element no.	Design variables, cm	Modal approx. 60% M.L. Peak time approximation type 1	2	3	Hybrid approx. 30% M.L.
	B	25.00	25.00	25.00	25.00
1	H	25.00	25.00	25.00	25.00
	T	0.33	0.36	0.34	0.27
	B	11.11	11.75	11.40	12.72
2	H	10.01	10.64	10.52	14.21
	T	0.15	0.16	0.17	0.19
	B	17.76	24.57	19.23	24.79
3,4	H	24.35	20.55	24.89	24.89
	T	0.36	0.35	0.35	0.36
	B	25.00	23.71	24.59	24.78
5,6	H	16.66	15.85	14.36	24.81
	T	0.38	0.37	0.40	0.42
	B	14.67	13.37	17.01	12.22
7,8	H	15.46	15.30	15.52	19.18
	T	0.10	0.11	0.10	0.10
Dampers	c	1.76	1.65	1.67	1.30
Mass, kg		284	290	290	317
Number of analyses		14	14	12	26

resulting in the total of 18 degrees of freedom. Two dampers with a mass of 4 kg are attached to nodes 5 and 7. These dampers are oriented so that the force they generate acts in the vertical direction. Two independent load conditions with homogeneous initial conditions are considered for this problem. The first load condition consists of a transient vertical force $f_1(t)$ and a transient moment $f_2(t)$ in the x direction at node 3. Note that this loading will excite both bending and torsion in the structure. These loads are given by $f_1(t) = 333.3t$ N and $f_2(t) = 10 \times f_1(t)$ N · cm for $0 \leq t \leq 0.3$ s and $f_1(t) = f_2(t) = 0$ for $t > 0.3$ s (see Fig. 6). Transient response is considered for the time interval $0 \leq t \leq 2$ s, and 20 out of the 36 complex modes are used to calculate the peak response values. The second load condition consists of a harmonic force and moment at the same location and direction as the first load case. These loads are given by $f_1(t) = 400\,\text{N} \sin \Omega t$ and $f_2(t) = 10 \times f_1(t)$ N · cm with $\Omega = 3.9$ Hz.

Structural elements are linked to produce a symmetric structure with respect to the x–y plane. Each beam element has three design variables (B, H, and T), with initial design $B = H = 20.0$ cm

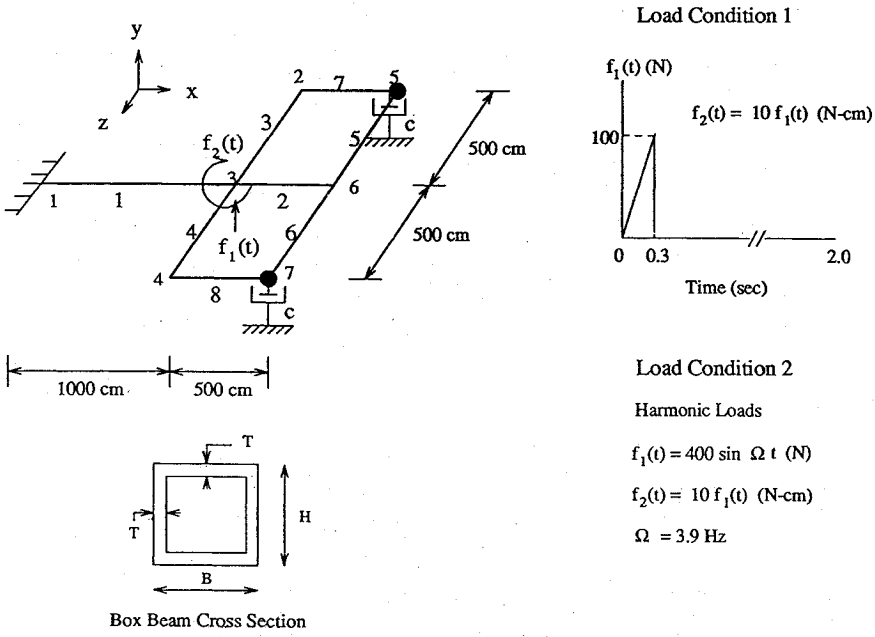

Fig. 6 Antenna structure, problem 2.

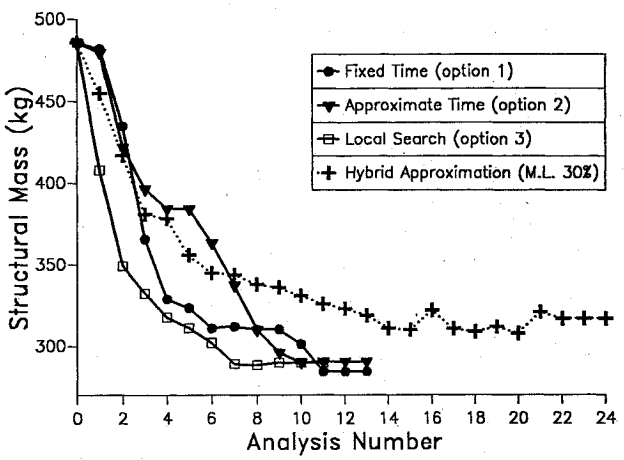

Fig. 7 Iteration histories of antenna structure.

and $T = 0.5$ cm, and side constraints 10.0 cm $\leq B, H \leq 25.0$ cm, and 0.1 cm $\leq T \leq 1.0$ cm. The damping coefficients are also linked with an initial value of $c = 1$ N · s/cm and no side constraints. Dynamic displacements in the y direction at nodes 2, 4, 5, and 7 are constrained to be less than or equal to 1.0 cm and damper forces to be less than or equal to 8.5 N. Move limits of 60% are used for this problem.

Approximations for the frequency response from the second load condition are based on Ref. 6. The cross-sectional area and inertias are used as intermediate design variables for structural elements and the damping coefficient for dampers. Three runs were made for this problem, each one corresponding to the different peak time approximation option. Iteration histories are given in Fig. 7 and final designs in Table 3. From Table 3 it is observed that in all cases the final designs converge within a range of 2% difference between final objective function values. Simple first-order approximations were also used to solve this problem. Within move limits between 20 and 50%, convergence was achieved only with hybrid approximations with 30% move limits and 24 design cycles. The iteration history data for this run are given in Fig. 7 and final design in Table 3. It is observed that using hybrid approximations not only requires more structural analyses for convergence, but the final mass (317 kg) is 9% higher than the final mass using the improved modal approximation (290 kg).

Conclusions

A new approximation for peak transient displacements based on modal analysis has been presented. This approximation allows the use of larger move limits as compared with traditional first-order approximations. Using larger move limits reduces the number of structural analyses and therefore reduces the computational cost associated with the synthesis process. It is important to note that when transient response constraints are considered, reducing the number of analyses becomes of great importance, since for real applications the computational burden of transient analysis is very large.

In constructing explicit approximations for peak transient dynamic response constraints, the use of intermediate response quantities and intermediate design variables has been extensively exploited. It should be recognized that the choice of the intermediate design variables depends on the type of structural element used in the design process. In this work the intermediate response quantities U_r, T_r, S_r, TD_r, SD_r, and TV_r were approximated linearly in terms of the intermediate design variables, but a hybrid expansion can be used if more conservative approximations are required.

The different options for peak time approximations show a similar behavior. In all cases it was observed from the example problems that using a local search gives a more accurate approximation for the peak time, but this is not necessarily reflected in the convergence characteristics. The most inexpensive option, from a computations point of view, is to keep the peak times invariant for each approximate problem, and the convergence characteristics are similar to the other options. Thus, this option should be used as a default unless a more accurate approximation for the peak time itself is required.

Finally, the disjointness of the design space that occurs when constraints are placed on dynamic response[13–17] is captured by modal approximations. This makes it possible to attack the global optimization problem by using some kind of global optimizer to solve the approximate problem[15,17] or some other kind of heuristic methods such as the ones presented in Refs. 16 and 18 for frequency response.

References

[1]Schmit, L. A., and Farshi, B., "Some Approximation Concepts for Efficient Structural Synthesis," *AIAA Journal*, Vol. 12, No. 5, 1974, pp. 692–699.

[2]Schmit, L. A., and Miura, H., "Approximation Concepts for Efficient Structural Synthesis," NASA CR 2552, March 1976.

[3]Vanderplaats, G. N., and Salajegheh, E., "A New Approximation Method for Stress Constraints in Structural Synthesis," *AIAA Journal*, Vol. 27, No. 3, 1989, pp. 352–358.

[4]Canfield, R. A., "An Approximation Function for Frequency Constrained Structural Optimization," *AIAA Journal*, Vol. 28, No. 6, 1990, pp. 1116–1122.

[5]Thomas, H. L., Sepulveda, A. E., and Schmit, L. A., "Improved Approximations for Dynamic Displacements Using Intermediate Response Quantities," *Proceedings of the 3rd NASA/Air Force Symposium on Recent Advances in Multidisciplinary Analysis and Optimization* (San Francisco, CA), 1990, pp. 95–104.

[6]Sepulveda, A. E., and Thomas, H. L., "A New Approximation for Steady-State Response of General Damped Systems," *AIAA Journal*, Vol. 33, No. 6, 1995, pp. 1127–1133.

[7]Thomas, H. L., Sepulveda, A. E., and Schmit, L. A., "Improved Approximations for Control Augmented Structural Optimization," *AIAA Journal*, Vol. 30, No. 1, 1992, pp. 171–179.

[8]Sepulveda, A. E., Thomas, H. L., and Schmit, L. A., "Improved Transient Response Approximations for Control Augmented Structural Optimization," *Proceedings of the 2nd Pan American Congress of Applied Mechanics* (Valparaiso, Chile), UTFSM, Valparaiso, Chile, 1991, pp. 611–614.

[9]Barthelemy, J. F. M., and Haftka, R. T., "Approximation Concepts for Optimum Structural Design—A Review," *Structural Optimization*, Vol. 5, No. 3, 1993, pp. 129–144.

[10]Grandhi, R. V., Haftka, R. T., and Watson, L. J., "Design-Oriented Identification of Critical Times in Transient Response," *AIAA Journal*, Vol. 24, No. 4, 1986, pp. 649–656.

[11]Vanderplaats, G. N., "DOT Users Manual," Version 4.00, VMA Engineering, Colorado Springs, CO, 1993.

[12]Starnes, J. H., and Haftka, R. T., "Preliminary Design of Composite Wings for Buckling, Stress, and Displacement Constraints," *Journal of Aircraft*, Vol. 16, 1979, pp. 564–570.

[13]Cassis, J. H., "Optimum Design of Structures Subjected to Dynamic Loads," School of Engineering and Applied Science, Univ. of California, Los Angeles, UCLA-ENG-7451, Los Angeles, CA, June 1974.

[14]Johnson, E. H., "Disjoint Design Spaces in the Optimization of Harmonically Excited Structures," *AIAA Journal*, Vol. 14, No. 2, 1976, pp. 259–261.

[15]Sepulveda, A. E., and Schmit, L. A., "Approximation Based Global Optimization Strategy for Structural Synthesis," *AIAA Journal*, Vol. 31, No. 1, 1993, pp. 180–188.

[16]Mills-Curran, W. C., and Schmit, L. A., "Structural Optimization with Dynamic Behavior Constraints," *AIAA Journal*, Vol. 23, No. 1, 1985, pp. 131–138.

[17]Sepulveda, A. E., and Jin, I. M., "Design of Structure/Control Systems with Transient Response Constraints Exhibiting Relative Minima," *Proceedings of the AIAA/USAF/NASA/OAI 4th Symposium on Multidisciplinary Analysis and Optimization* (Cleveland, OH), AIAA, Washington, DC, 1992, pp. 371–378.

[18]Miura, H., and Chargin, M., "Automated Tuning of Airframe Vibration by Structural Optimization," *Proceedings of the 42nd Annual Forum and Display*, American Helicopter Society, Washington, DC, 1986.